Experimental Evaluation of the Composite Behavior of Precast Concrete Sandwich Wall Panels

Stephen Pessiki, Ph.D.
Associate Professor
Department of Civil and Environmental Engineering
Lehigh University
Bethlehem, Pennsylvania

Alexandar Mlynarczyk
Project Engineer
Wiss, Janney, Elstner Associates
Princeton Junction, New Jersey

Lateral load tests were performed on four full-scale precast concrete sandwich wall panels. The first panel was a typical precast, prestressed concrete sandwich panel that had shear transfer provided by regions of solid concrete in the insulation wythe, metal wythe connectors (M-ties), and bond between the concrete wythes and the insulation wythe. The degree of composite action developed by each shear transfer mechanism (regions of solid concrete, wythe connectors, and bond) was then evaluated by testing three additional panels that included only one mechanism each. The panels were tested in a horizontal position with simple supports under the action of a uniform lateral pressure. It was found that, for the panel geometries and materials treated in this study, the solid concrete regions provide most of the strength and stiffness that contribute to composite behavior. Steel M-tie connectors and bond between the insulation and concrete contribute relatively little to composite behavior. For design purposes, it is recommended that solid concrete regions be proportioned to provide all of the required composite action in a precast sandwich wall panel.

A typical precast concrete sandwich wall panel is composed of two wythes of concrete separated by a wythe of insulation. Concrete wythes can be flat slabs, double tees, or other shape and may provide the structure with an architectural finish. Sandwich panels provide a versatile and economical means to meet the structural, thermal, and architectural requirements of a structure. For this reason, sandwich panels are used as exterior and interior walls for many types of structures.

Depending on load demands, sandwich panels may be prestressed or nonprestressed. Panels can be load-bearing, supporting gravity loads such as roof and floor loads, or nonload-bearing, transmitting wind and seismic loads to the structural frame and foundation.

Sandwich panels can be designed to behave compositely, where the two concrete wythes act together structurally, or noncompositely, where each concrete wythe acts independently. More commonly, however,

sandwich panels are designed semi-compositely, whereby varying degrees of composite action are assumed at stripping, handling, and service. To ensure sufficient composite action to meet strength and stiffness requirements, the designer must provide adequate shear transfer between concrete wythes.

In a typical sandwich panel, shear transfer may be provided through several different mechanisms, including: 1) solid concrete regions (i.e., regions where the insulation is intentionally omitted and replaced with concrete); 2) mechanical connectors that pass through the insulation wythe and into the concrete; and 3) bond between the concrete wythes and the insulation.

This paper investigates the flexural behavior of sandwich panels and the contribution to composite action provided by regions of solid concrete, mechanical wythe connectors, and bond.

Tests were performed on four full-scale sandwich panels. The first panel included regions of solid concrete in the insulation wythe, metal wythe connectors, and bond between the concrete and insulation wythes. The degree of composite action developed by each of the three shear transfer mechanisms was then evaluated by testing three additional panels that included only one mechanism of shear transfer each. Comparisons of the behavior of each panel provided information about the contribution to composite action provided by the three shear transfer mechanisms.

The work described in this paper is part of an ongoing research program at Lehigh University on precast concrete sandwich wall panels. The work aims to provide recommendations for the design of sandwich wall panels and explores the development of new types of sandwich panels with improved thermal and structural performance.

BACKGROUND

Much of the knowledge on sandwich panel behavior is based on observed field performance and laboratory testing. Because of the limited amount of data available, there is a general lack of agreement among designers on the degree of composite action provided by shear transfer mechanisms and resulting panel performance. Much of the present information on the behavior and design of sandwich panels is provided in several recent reports.[1-3]

A fully composite sandwich panel is one in which the two concrete wythes act integrally to resist bending. In theory, a fully composite panel exhibits plane section behavior throughout its entire depth at all locations along its span. Full composite action is achieved by providing sufficient horizontal shear transfer between wythes.

A noncomposite sandwich panel is one in which each concrete wythe acts independently to resist bending. Plane section behavior is obtained in each wythe, but not through the entire panel depth.

A partially composite panel is one in which concrete wythes act at least partly together to resist bending. Thus, a partially composite panel resists bending to a degree between that of a fully composite panel and a noncomposite panel. Einea et al.[1] defined a partially composite panel as a panel in which the connectors can transfer between zero and 100 percent of the longitudinal shear required for a fully composite panel.

Finally, the degree of composite action exhibited by a panel may change throughout the loading history of the panel. For example, a panel may start out being fully composite, but under the action of increasing load, time, and temperature variation, the different mechanisms that contribute to composite action may degrade.

Wythe Connectors

According to the PCI State-of-the-Art Report,[2,3] two types of connectors are used to construct sandwich panels; these are nonshear connectors and shear connectors.

Nonshear connectors transfer normal tension forces between the concrete wythes to prevent the wythes and insulation from separating during stripping and handling. These come in several forms, including metallic and fiber composite pin connectors, and transverse welded wire ladder connectors.

Shear connectors transfer both horizontal shear forces and normal tension forces between the wythes. There are two different types of shear connectors:

- One-way shear connectors are stiff in one direction and flexible in the other. Often these connectors are used to resist shear in the longitudinal direction of the panel. According to the PCI report,[2,3] typical one-way shear connectors include M-ties and welded wire trusses.
- Other shear connectors are stiff in at least two directions and resist both longitudinal and transverse shears. These connectors include solid blocks of concrete and cylindrical sleeve anchors.

Previous Tests of Sandwich Panels

Pfeifer and Hanson[4] tested approximately 50 nonprestressed sandwich panels with a variety of wythe connectors in flexure under uniform loading. The test panels measured 5 x 3 ft (1.52 x 0.91 m), with thicknesses ranging from 2.25 to 6 in. (57 to 152 mm). It was found that by varying the types of connectors and their spacing, varying degrees of composite action could be achieved. Metal connectors with diagonal members, such as a welded wire truss, were more effective in transferring shear than those without diagonal members. It was also discovered that concrete ribs provided better shear transfer than metal connectors.

Bush and Stine[5,6] tested six precast concrete sandwich panels with continuous truss connectors. The primary variables of the test program included the number, orientation, and spacing of the connectors. Each test panel measured 16 x 8 ft (4.88 x 2.44 m) and was tested under uniform lateral pressure. Each panel was 8 in. (203 mm) thick and comprised two 3 in. (76 mm) thick concrete wythes and a 2 in. (51 mm) thick insulation wythe. The tests showed that a high degree of composite stiffness and flexural capacity could be achieved with truss connectors oriented longitudinally in the panels.

The tests also revealed that a signifi-

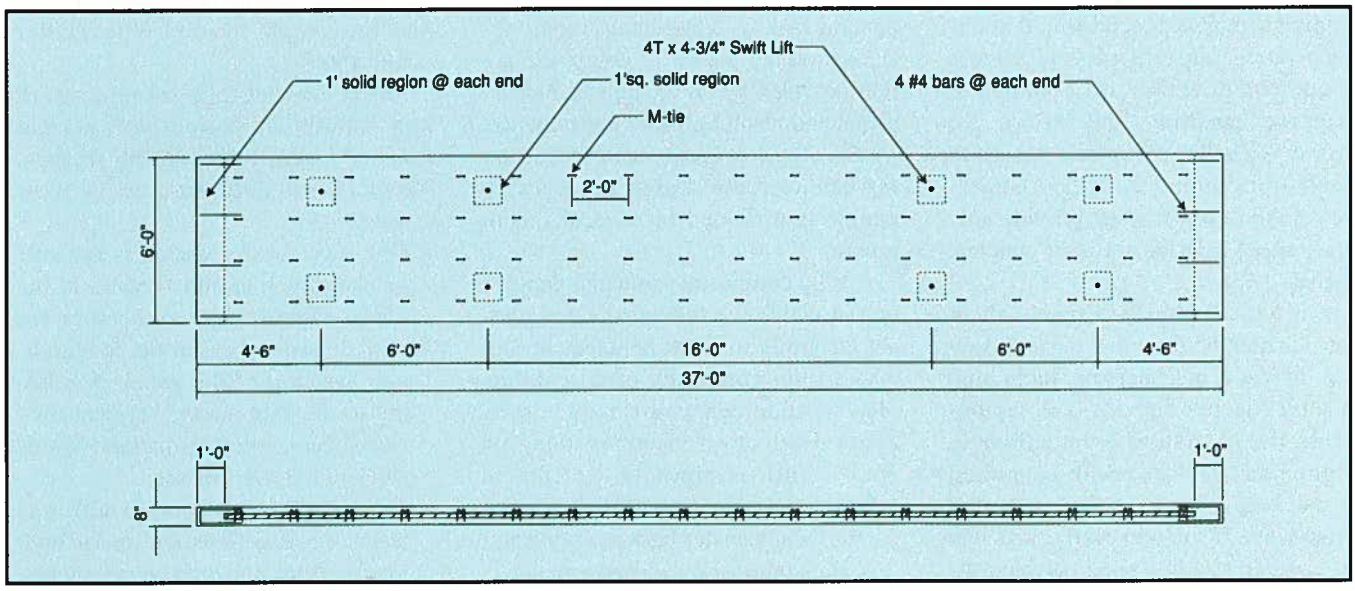

Fig. 1. Plan view and longitudinal section of Panel 1 (Note: 1 in. = 25.4 mm; 1 ft = 0.3048 m).

Table 1. Experimental program.

Panel	M-tie connector	Concrete–insulation bond	Solid regions of concrete	Primary variable
1	Yes	Yes	Yes	Prototype panel
2	Yes	No	No	Fraction of composite action provided by M-tie connector
3	No	No	Yes	Fraction of composite action provided by solid concrete regions
4	No	Yes	No	Fraction of composite action provided by bond between insulation and concrete

cant amount of shear was transferred through stripping and handling inserts, as well as through solid concrete ribs. It was further shown that friction bond between insulation and concrete provided a modest contribution to the overall shear transfer.

EXPERIMENTAL PROGRAM

The testing program, outlined in Table 1, was designed to investigate the degree of composite action contributed by each of the three mechanisms described previously. Four panels were tested in all. Panel 1, the prototype panel, was designed and fabricated as a panel that might be for commercial use. This panel contained all three shear transfer mechanisms, with metal M-ties used as the mechanical connectors. Each of the three remaining panels had only one mechanism of shear transfer; this was done to isolate and quantify each mechanism's independent contribution to the development of composite action.

Test Panel Details

Each panel was 8 in. (203 mm) thick and comprised of two 3 in. (76 mm) concrete wythes and a 2 in. (51 mm) insulation wythe. Each panel measured 6 ft wide x 37 ft long (1.83 x 11.28 m) and spanned 35 ft (10.67 m) simply supported. For all panels, each concrete wythe was axially prestressed with four $^{7}/_{16}$ in. (11 mm) diameter Grade 270 low-relaxation steel prestressing strands. Each wythe also contained No. 3 Grade 60 reinforcing bars placed transversely at 2 ft (0.61 m) on center. Design concrete compressive strength was 3500 psi (24.1 MPa) at transfer and 6000 psi (41.4 MPa) at 28 days.

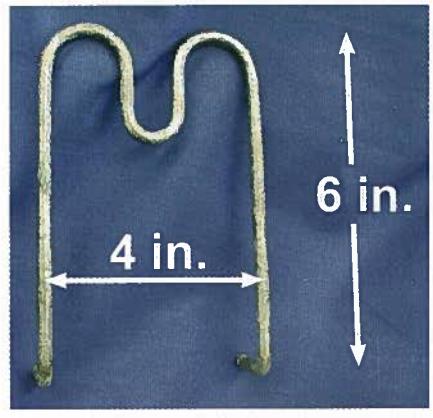

Fig. 2. Steel M-tie connector.

Fig. 1 shows the details of Panel 1. This panel contains a 1 ft (0.30 m) wide solid band of concrete at each end. There are also eight 1 ft (0.30 m) square solid regions located throughout the span of the panel to provide locations for placement of lifting hardware. Steel M-tie connectors (Fig. 2) are spaced at 2 ft (0.61 m) on center. No attempt was made to influence the bond between the concrete wythes and the insulation.

Appendix B provides the design calculations for Panel 1. Table 2 presents a summary of the key design parameters for this panel. Panel 1 was designed according to the ACI Building Code (ACI 318-99),[7] the PCI Design Handbook,[8] and the "Guide for Precast Concrete Wall Panels" (ACI 533R-93).[9] Panel 1 was designed as a partially composite panel, with full composite action assumed for stripping and han-

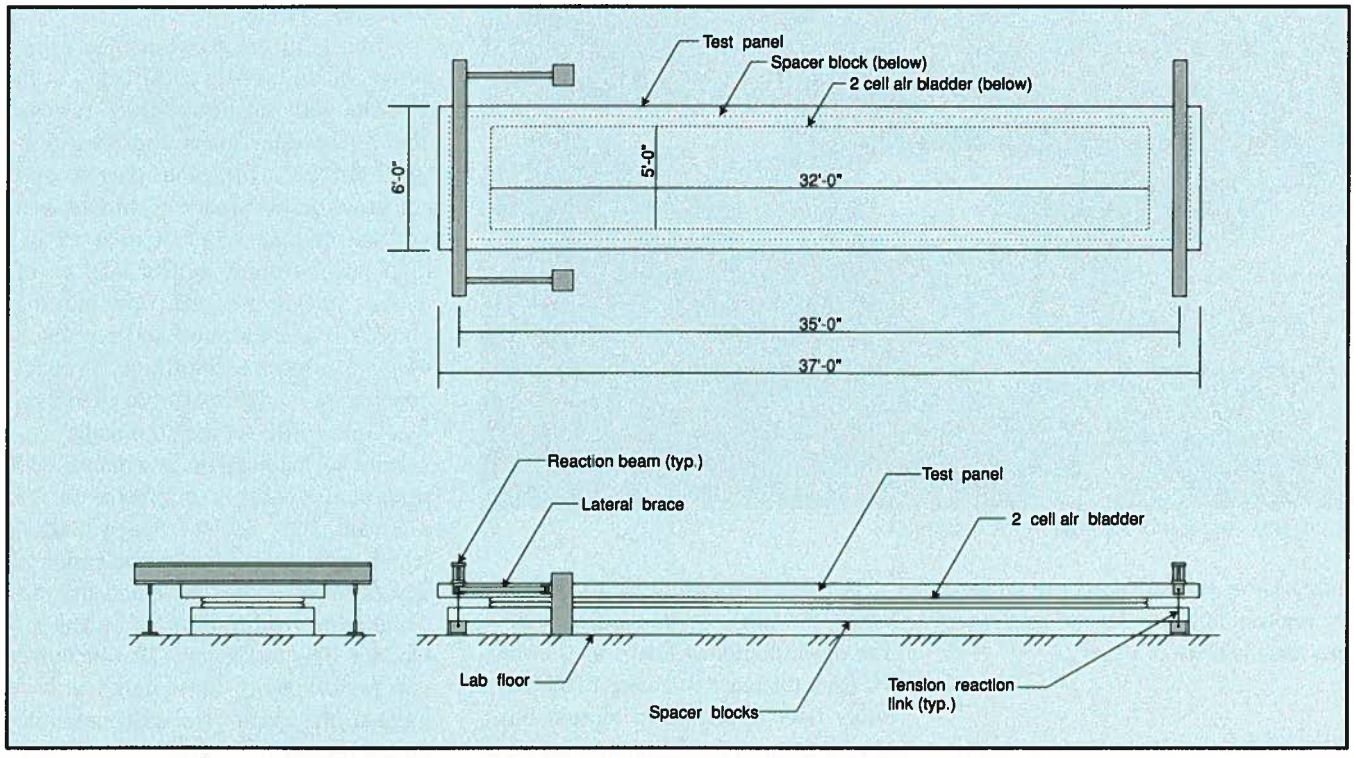

Fig. 3. Test fixture (Note: 1 in. = 25.4 mm; 1 ft = 0.3048 m).

dling and 70 percent composite action assumed for service.

Panel 2 was designed to investigate the fraction of composite action provided by the steel M-tie connectors. This panel contained no solid concrete regions, and the bond between the concrete wythes and the insulation was eliminated by a plastic bond breaker at each concrete-insulation interface. The steel M-ties were spaced at 2 ft (0.61 m) on center, using the same configuration as Panel 1. The lifting hardware was embedded in only the face wythe, and this hardware was removed during testing to prevent shear transfer from occurring at the lifting points. There were no full-depth regions of solid concrete at the lifting points.

Panel 3 was designed to investigate the fraction of composite action provided by the solid concrete regions. This panel contained no M-tie connectors, and the bond between the concrete wythes and the insulation was eliminated by a plastic bond breaker. Solid concrete regions were provided using the configuration, reinforcement, and lifting hardware equivalent to Panel 1.

Panel 4 was designed to investigate the fraction of composite action provided by the bond between the concrete wythes and the insulation. This panel contained

Table 2. Summary of key design parameters.

Dimensions	Width, b	6 ft
	Overall length, L'	37 ft
	Span length, L	35 ft
	Concrete wythe thickness	3 in.
	Insulation thickness	2 in.
	Total thickness	8 in.
Section properties	A_c (both wythes)	432 in.^{2}
	I (fully composite), I_c	3024 in.^{4}
	S (fully composite), S_c	756 in.^{3}
	I (fully noncomposite), I_{nc}	324 in.^{4}
	S (fully noncomposite), S_{nc}	216 in.^{3}
Prestress properties	A_p	0.92 in.^{2}
	e_p	0 in.
	E_p	28,500 ksi
	f_{pu}	270 ksi
	$f_{pi} = 0.70 f_{pu}$	189 ksi
	P_i	174 kips
	R (assumed)	0.87
	P_e	151 kips
	f_{pe}	0.35 ksi
Concrete properties	f'_{ci}	3500 psi
	E_{ci}	3370 ksi
	f'_c	6000 psi
	E_c	4415 ksi

Note: 1 in. = 25.4 mm; 1 ft = 0.3048 m; 1 in.^{2} = 645 mm^2; 1 kip = 4.448 kN; 1 ksi = 1000 psi = 6.895 MPa.

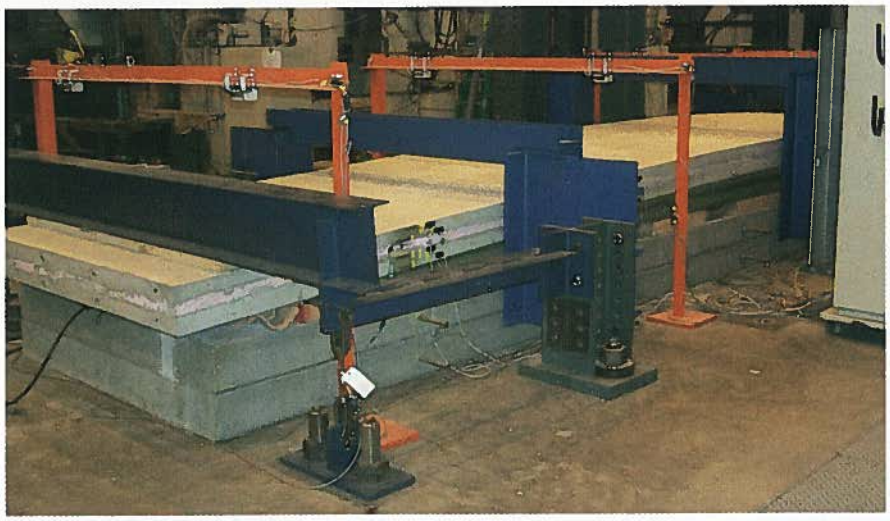

Fig. 4. Photograph of a panel in the test fixture.

neither M-ties nor solid concrete regions, and removable lifting inserts used were equivalent to those of Panel 2.

Test Fixture

Fig. 3 is a drawing of the test fixture, and Fig. 4 is a photograph of a panel in the fixture during a test. Each panel was tested in a horizontal position, with simply supported end conditions. Lateral loading was applied from beneath the panel as uniform pressure, and no axial load was applied.

Each panel spanned 35 ft (10.67 m) center-to-center of the reaction beams. The upward applied load was transmitted from the reaction beams to the laboratory floor through four tension links, one at each end of the two reaction beams. The tension links were instrumented with load cells to measure the upward force applied to the panel.

At one end of the span, longitudinal movement of the panel was restrained to simulate a pinned end condition. Longitudinal movement of the panel was permitted at the opposite end, simulating a roller support.

Uniform pressure was applied using a two-cell air bladder constructed from a rubber-coated heavy-duty fabric. The air bladder measured 32 x 5 ft (9.75 x 1.52 m) in plan. Its two-cell construction allowed it to inflate to a vertical displacement of over 12 in. (305 mm) without significant loss of contact surface area. Air flow into the bladder was monitored and regulated using a pressure regulator. Precast concrete spacer blocks were used as a reaction surface for the air bladder.

Prior to loading, the test panel was supported around its perimeter on 3.5 x 3.5 in. (89 x 89 mm) wood blocks, which were set on top of the concrete spacer blocks. This prevented the test panel from resting directly on the air bladder. The test fixture also included several braces to limit panel movement in the event of a sudden failure during testing.

Instrumentation

All test panels were instrumented as shown in Fig. 5. Load cells in the steel tension links were used to measure the force P applied to the panel. Displacement potentiometers were attached to

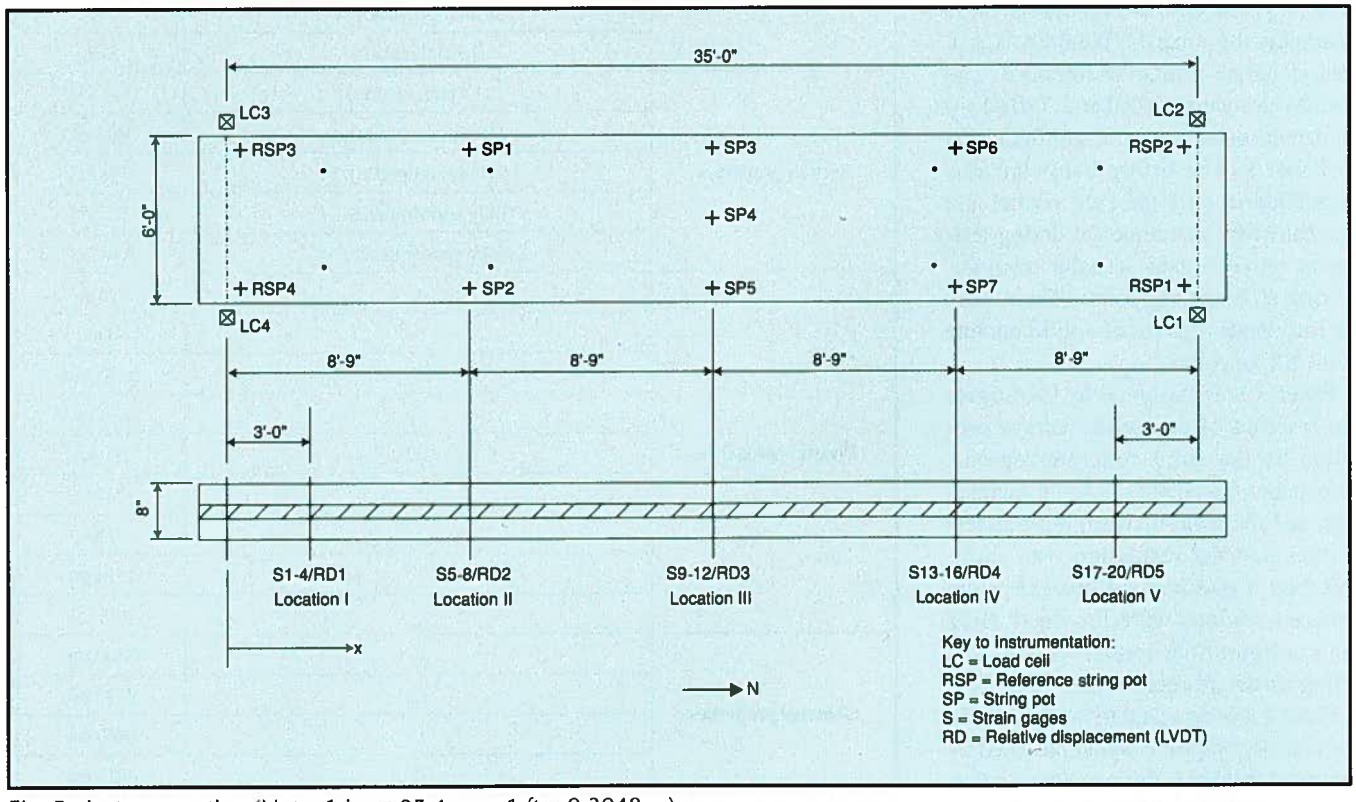

Fig. 5. Instrumentation (Note: 1 in. = 25.4 mm; 1 ft = 0.3048 m).

the back wythe to measure lateral displacements under load. Lateral displacements were measured at the panel quarter points and at midspan. In addition, four reference displacements were measured, one at each panel corner. These reference measurements were necessary because the panel experienced a small amount of vertical displacement until the tension links began to engage and take on load. This vertical displacement occurred as the applied pressure equilibrated the self-weight of the panel. These values formed a reference for all other displacement measurements.

Relative displacement between the two concrete wythes was monitored using linear variable differential transformers (LVDTs). The LVDTs were placed at five locations along the span of the panel. A small amount of insulation was removed where each LVDT was located between the concrete wythes.

Electrical resistance strain gauges were used to measure the distribution of strain through the thickness of the panel. The gauges were placed at the same locations as the LVDTs described above. At each location, two gauges were attached to the back wythe, and two gauges were attached to the face wythe. All four gauges were placed on the sides of the wythes. Since only two gauges were used on each wythe, plane section behavior is assumed within each individual wythe, and the strain measurements were intended to evaluate plane section behavior throughout the entire panel thickness.

Loading Procedure

Panel 1 was tested first. The loading procedure for Panels 2 to 4 was modified slightly after Panel 1 was tested. For Panel 1, as self-weight was equilibrated by the upward pressure in the air bladder, the panel experienced a small amount of lift-off from its wood supports before engaging the tension links against the laboratory floor.

During lift-off, the panel was not subjected to a completely uniform load along its length because the air bladder was only 32 ft (9.75 m) long, whereas the test panel was 37 ft (11.28 m) long.

Table 3. Concrete material properties.

Panel	Age at testing (days)	Face wythe		Back wythe		Average of face and back wythes	
		f'_c (psi)	E_c (ksi)	f'_c (psi)	E_c (ksi)	f'_c (psi)	E_c (ksi)
1	30	7050	4790	6820	4710	6930	4750
2	28	8340	5210	9170	5460	8760	5340
3	175	8000	5100	4480	3820	6240	4500
4	152	7480	4930	6510	4600	7000	4770

Note: 1 ksi = 1000 psi = 6.895 MPa.

This created an unsupported length of 2.5 ft (0.76 m) at each end of the panel. This unsupported self-weight, along with the weight of the reaction beams and other test fixture hardware, caused some bending of the panel before the tension links were fully engaged.

In the data reduction for Panel 1, the values of load were adjusted to account for the additional load that was initially applied to the panel by the self-weight of the unsupported length of panel and the test fixture. Specifically, the self-weight of the unsupported panel and the self-weight of the test fixture were added to the total applied lateral load. For Panel 1, this value was 3250 lbs (14.5 kN). Since the panel was still in the uncracked, linear elastic range, the data were easily extrapolated back to the origin of the load-deflection plot.

The test procedure was modified slightly for the remaining three panels because there was concern that they may not remain uncracked during the lift-off part of the loading. The initial moment created by the unsupported panel self-weight and the fixture self-weight was eliminated by applying an upward point load at each end of the panel using a hydraulic jack placed at mid-width of the panel directly beneath the reaction beam.

The upward point load applied to each panel was calculated based on the fixture weight and the unsupported panel self-weight. These values were 3000, 3250, and 3000 lbs (13.3, 14.5, and 13.3 kN) for Panels 2, 3, and 4, respectively. All loading values presented in the remainder of this paper include the adjustments for panel weight and test fixture weight as described above. In the modified test procedure, the hydraulic pump was turned on to apply the point loads to the ends of the panel, and then the lateral load was applied by filling the air bladder.

None of the four test panels exhibited failure by crushing of the concrete in the compression zone in flexure. Instead, all test panels became increasingly more flexible as the tests progressed to the point where midspan deflection continued to increase with relatively little increase in resistance. Loading was stopped when the maximum midspan deflection of the panels reached approximately 9 in. (230 mm).

Material Properties

Concrete compressive strength was determined from compression tests of 6 x 12 in. (152 x 305 mm) field-cured cylinders. For each test panel, three cylinders from the face wythe concrete and three cylinders from the back wythe concrete were prepared according to ASTM C 31 procedures using plastic molds; these were cured under the same conditions as the sandwich panels.

The cylinders were tested at approximately the same age that the corresponding panel was tested. The cylinders were capped with a sulfur mortar compound according to ASTM C 617 and tested according to ASTM C 39. The results of the cylinder tests for all four panels are presented in Table 3. The modulus of elasticity, E_c, computed as $57{,}000\sqrt{f'_c}$, is also presented.

Material properties for the prestressing strand were taken from the PCI Handbook[8] as follows: yield stress f_{py} = 243 ksi (1675 MPa), ultimate strength f_{pu} = 270 ksi (1862 MPa), and modulus of elasticity E_p = 28,500 ksi (196.5 GPa).

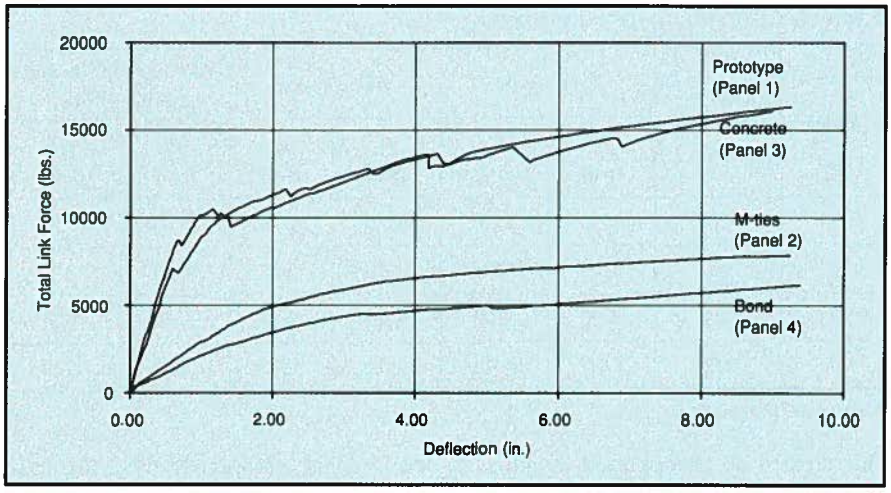

Fig. 6. Load versus deflection for all test panels (Note: 1 in. = 25.4 mm; 1 lb = 4.448 N).

All test panels were made using an extruded polystyrene rigid foam insulation. Material strengths from the manufacturer were as follows: minimum compressive strength = 25 psi (172 kPa), minimum flexural strength = 75 psi (517 kPa), and modulus of elasticity = 1.35 ksi (9.3 MPa).

The steel M-tie connectors in Panels 1 and 2 measured 6 x 4 in. (152 x 102 mm), and were formed from 0.25 in. (6.4 mm) galvanized steel wire (see Fig. 2).

RESULTS AND DISCUSSION

A summary of the experimental results is presented here. A complete presentation of the results is given in References 10 and 11. For simplicity in identifying the test panels, from this point forward all test panels are identified by their mechanism of shear transfer. Panel 1 is identified as the Prototype Panel, which contained all three mechanisms of shear transfer; Panels 2, 3, and 4 are identified as the M-tie Panel, Concrete Panel, and Bond Panel, respectively.

Load-Deflection Behavior

Fig. 6 shows the load-deflection response of the four test panels. The Prototype Panel behaved in a linear elastic manner up to a load of P = 8710 lbs (38.7 kN) and a midspan lateral deflection of Δ = 0.68 in. (17 mm). The first flexural crack was observed at this point. In general, the formation of each flexural crack was associated with a distinct drop in load in the load-deflection plot.

This panel showed a dramatic reduction in stiffness, upon formation of the second flexural crack, at a load of P = 10,490 lbs (46.7 kN) and a lateral deflection of Δ = 1.16 in. (30 mm). Deflection increased much more rapidly for a given increase in load beyond this point. The panel was loaded up to a maximum load of P = 16,340 lbs (72.7 kN) and a lateral deflection of Δ = 9.26 in. (235 mm). The test was terminated at this point and the panel was unloaded.

The Concrete Panel exhibited load-deflection behavior similar to the Prototype Panel. As shown in Fig. 6, the initial stiffness of the Concrete Panel was slightly less than the Prototype Panel. First cracking occurred at a load of 7080 lbs (31.5 kN), which is slightly lower than the load at which the Prototype Panel cracked.

The M-tie Panel exhibited a load-deflection behavior that was dramatically different from the Prototype and Concrete Panels. As shown in Fig. 6, its initial stiffness was much less than the Prototype and Concrete Panels. The first flexural crack formed at a load of 2890 lbs (12.9 kN). Unlike the Prototype and Concrete Panels, flexural cracks were not associated with distinct drops in load.

The Bond Panel exhibited behavior similar to the M-tie Panel, and it exhibited the smallest initial flexural stiffness of the four panels. The first flexural crack occurred at a load of 820 lbs (3.6 kN). Similar to the M-tie Panel, flexural cracks were not associated with distinct drops in load.

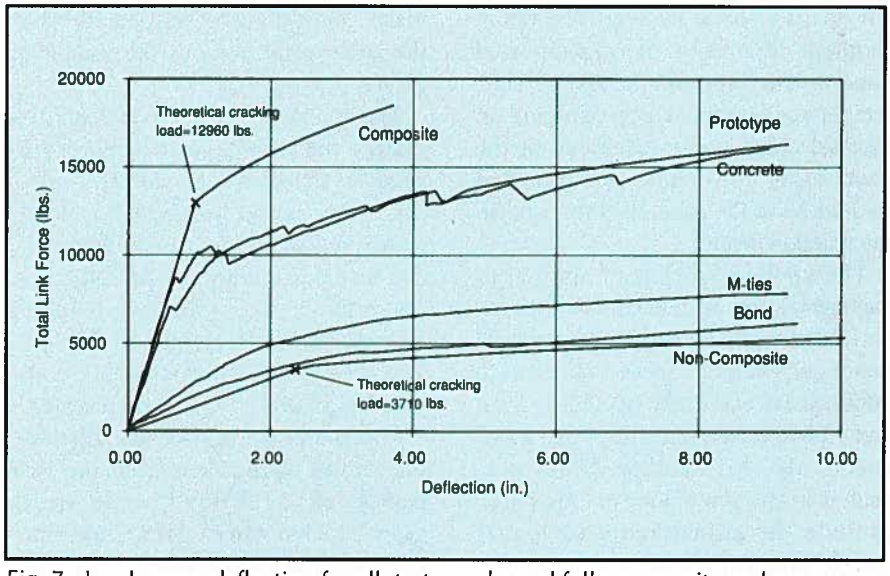

Fig. 7. Load versus deflection for all test panels, and fully composite and noncomposite panels (Note: 1 in. = 25.4 mm; 1 lb = 4.448 N).

Comparison of Experimental and Theoretical Load-Deflection Behavior

Fig. 7 compares the load-deflection behavior of the four test panels with theoretical load-deflection curves for fully composite and noncomposite panels. In computing the theoretical curves, E_c was computed using an unconfined concrete compressive strength of 7230 psi (49.9 MPa), which was the average strength of cylinder tests for all test panels.

Each of the theoretical composite and noncomposite curves consists of

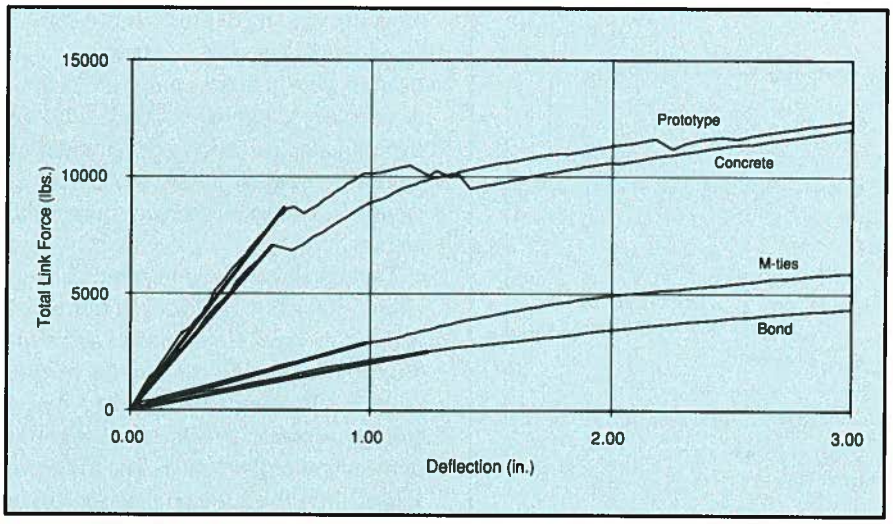

Fig. 8. Load versus deflection for all panels, and initial uncracked stiffnesses (Note: 1 in. = 25.4 mm; 1 lb = 4.448 N).

two parts. In the first part, the concrete is uncracked, and the moment of inertia is taken as I_g, the gross moment of inertia of the section. In calculating I_g for the composite section, the two wythes are assumed to act together to resist bending; for the noncomposite section, each wythe is assumed to act independently to resist bending.

The second part of each theoretical curve begins at the theoretical cracking load, which was P = 12,960 lbs (57.6 kN) and P = 3710 lbs (16.5 kN) for the composite and noncomposite curves, respectively, based on a concrete tensile strength of $f_r' = 7.5\sqrt{f_c'}$. These cracking loads, indicated in Fig. 7, correspond to equivalent wind loads of 67.5 and 19.3 psf (3.2 and 0.9 kPa) for composite and noncomposite panels, respectively. These pressures are computed from the load and the full 6 ft (1.83 m) panel width and 32 ft (9.75 m) bladder length.

After cracking, the theoretical deflection is computed using the effective moment of inertia, I_e. For partially cracked prestressed beams, I_e is given by Nilson[12] as:

$$I_e = \left(\frac{M_{cr}}{M_a}\right)^3 I_g + \left[1 - \left(\frac{M_{cr}}{M_a}\right)^3\right] I_{cr} \quad (1)$$

where

I_g = moment of inertia of the gross concrete section

I_{cr} = moment of inertia of fully cracked transformed concrete section

M_{cr} = cracking moment

M_a = maximum moment acting in the span

In Fig. 7, the theoretical curve for the composite panel is terminated at the point that the concrete becomes nonlinear (assumed to be at $0.5 f_c'$).

The observation that the Prototype and Concrete Panels cracked at load values well below the predicted cracking load, even though they appeared to initially exhibit a behavior similar to fully composite panels, is discussed further in the paper.

Initial Uncracked Stiffnesses

Fig. 8 is a plot of load versus deflection for all test panels, plotted up to a deflection value of 3.00 in. (76 mm). Superimposed on each curve is a straight line that represents the initial uncracked stiffness of each panel. For the Prototype, Concrete, and M-tie Panels, the initial uncracked stiffness was determined by extending a line from the origin to the point at which the first flexural crack occurred for each panel. Note that the line representing the initial uncracked stiffness for the Bond Panel was extended past the point at which the first flexural crack occurred [820 lbs (3.6 kN)], up to a load of 2520 lbs (11.2 kN), since the load-deflection curve remains relatively linear up to this point.

The straight lines which represent the initial uncracked stiffnesses for all test panels are replotted in Fig. 9. Two additional straight lines, representing the initial uncracked stiffnesses of theoretical fully composite and noncomposite panels, are also shown in the figure. The theoretical lines were discontinued at the point of the theoretical cracking load. As shown in the figure, the initial uncracked stiffnesses for all test panels fell within the region bounded by the initial uncracked stiffnesses for the theoretical composite and noncomposite panels.

Experimentally determined values of moment of inertia, I_{exp}, were computed as:

$$I_{exp} = \frac{5wL^4}{384\Delta E_c} \quad (2)$$

where

w = value of uniformly distributed load per length of panel

Δ = value of deflection that specifies the point which defines the line that represents the initial uncracked stiffness for each panel

The load w was calculated from total load P and the span length L of the test panel. The experimentally determined values of initial I_{exp} are presented in Table 4.

Composite Action

Of primary interest in this research program is the degree of composite action provided by each of the three shear

Table 4. Experimentally determined values of initial uncracked stiffness.

Panel type	P (lb)	w (lb/in.)	Δ (in.)	EI_{exp} (ksi)
Prototype	8710	22.7	0.64	14,360
Concrete	7080	18.4	0.59	12,660
M-tie	2890	7.5	0.98	3110
Bond	2520	6.6	1.24	2140

Note: 1 in. = 25.4 mm; 1 lb = 4.448 N; 1 kip = 4.448 kN; 1 ksi = 1000 psi = 6.895 MPa; 1 lb/in. = 175.1 N/m.

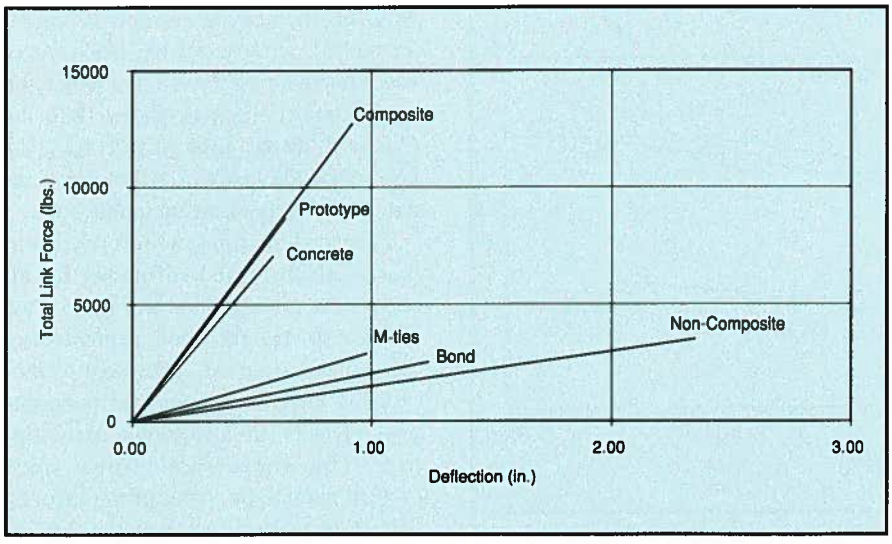

Fig. 9. Initial uncracked stiffnesses for all panels, including stiffnesses for theoretical fully composite and noncomposite panels (Note: 1 in. = 25.4 mm; 1 lb = 4.448 N).

transfer mechanisms. In this paper, the percent composite action, κ, achieved by each test panel is defined as:

$$\kappa = \frac{I_{exp} - I_{nc}}{I_c - I_{nc}}(100) \qquad (3)$$

where I_c and I_{nc} are the theoretical values of the fully composite and noncomposite moments of inertia of the panel. For the panels treated in this research, I_c = 3024 in.^{4} (1259 x 10^6 mm^4) and I_{nc} = 324 in.^{4} (135 x 10^6 mm^4).

Eq. (3) shows that the values of I_c and I_{nc} define the upper and lower bounds, respectively, of percent composite action. For example, if I_{exp}, the experimentally determined moment of inertia of a panel, is equal to I_c, then the panel exhibits 100 percent composite action. Conversely, if the experimentally determined moment of inertia of a panel is equal to I_{nc}, then the panel exhibits zero percent composite action. A partially composite panel, with an experimentally determined moment of inertia between I_c and I_{nc}, exhibits between 100 and zero percent composite action.

Table 5 shows the computed percent composite action, κ, for each test panel and for theoretical composite and noncomposite panels. As shown in this table, the Prototype Panel behaved as a fully composite panel, achieving 100 percent composite action. The Concrete Panel behaved nearly as a fully composite panel, achieving 92 percent composite action. In contrast, the M-tie and Bond Panels achieved only 10 and 5 percent composite action, respectively.

Relative Displacement Between Concrete Wythes

Fig. 10(a) is a plot of load versus relative displacement between concrete wythes for the Prototype Panel. Fig. 10(b) shows plots of load versus relative displacement for the Concrete and Prototype Panels plotted

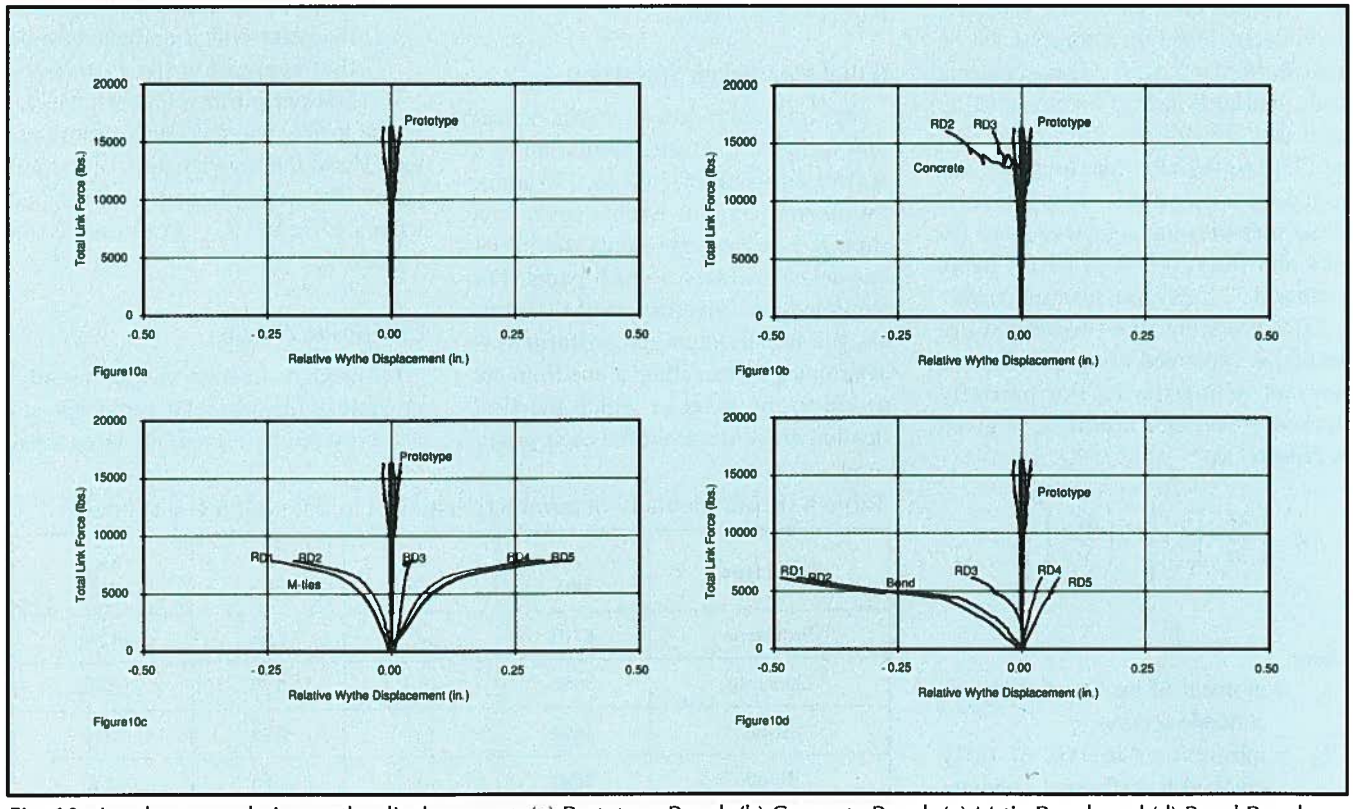

Fig. 10. Load versus relative wythe displacement: (a) Prototype Panel; (b) Concrete Panel; (c) M-tie Panel; and (d) Bond Panel (Note: 1 in. = 25.4 mm; 1 lb = 4.448 N).

Table 5. Computed percent composite action, κ, for all panels, including values for theoretical fully composite and noncomposite panels.

Panel type	EI_{exp} (ksi)	f'_c (psi)	E_c (ksi)	I_{exp} (in.^{4})	κ (%)
Composite	—	—	—	3024	100
Prototype	14,360	6930	4750	3024	100
Concrete	12,660	6240	4500	2814	92
M-tie	3110	8760	5340	583	10
Bond	2140	7000	4770	450	5
Noncomposite	—	—	—	324	0

Note: 1 ksi = 1000 psi = 6.895 MPa; 1 in.^{4} = 416231 mm^4.

together for comparison. Similarly, Figs. 10(c) and 10(d) show plots of load versus relative wythe displacement for the M-tie and Bond Panels plotted with the Prototype Panel results for comparison.

The Prototype Panel exhibited small values of relative displacements, which indicates a high degree of composite action during the test. Relative displacements were extremely small [less than 0.005 in. (0.13 mm)] while the panel remained within the linear elastic range. Upon formation of the second flexural crack, at a load of 10,490 lbs (46.7 kN), the flexural stiffness of the panel began to degrade significantly, and the values of relative displacement began to increase at a slightly faster rate with increasing load.

The Concrete Panel exhibited relative displacement behavior similar to that of the Prototype Panel. Relative displacements were extremely small while the panel remained within the linear elastic range.

Throughout its entire response, the M-tie Panel exhibited much larger values of relative displacement than the Prototype Panel. Values of relative displacement approached or exceeded 0.25 in. (6.4 mm) at both ends of the panel. Although it is likely that the M-ties provided some resistance to relative displacement, Fig. 10(c) shows that they are much less effective than regions of solid concrete.

The Bond Panel exhibited the largest values of relative displacement. The largest values, almost 0.5 in. (13 mm), occurred at Instruments RD1 and RD2. Relative displacements at the opposite end of the panel were much smaller, reaching a maximum of only 0.08 in. (2.03 mm) at Instrument RD5. Fig. 10(d) shows that bond contributes only a small amount of resistance to relative displacement, and that this resistance degrades rapidly with loading.

Concrete Strains

As explained earlier, a fully composite panel is expected to exhibit plane section behavior throughout its entire depth. The load-deflection results indicate that the Prototype and Concrete Panels behaved initially as fully or nearly fully composite panels. However, the measured strain distributions for the Prototype and Concrete Panels did not indicate plane section behavior through the depth of the panels.

To investigate this further, a linear elastic finite element analysis was performed to determine the distribution of

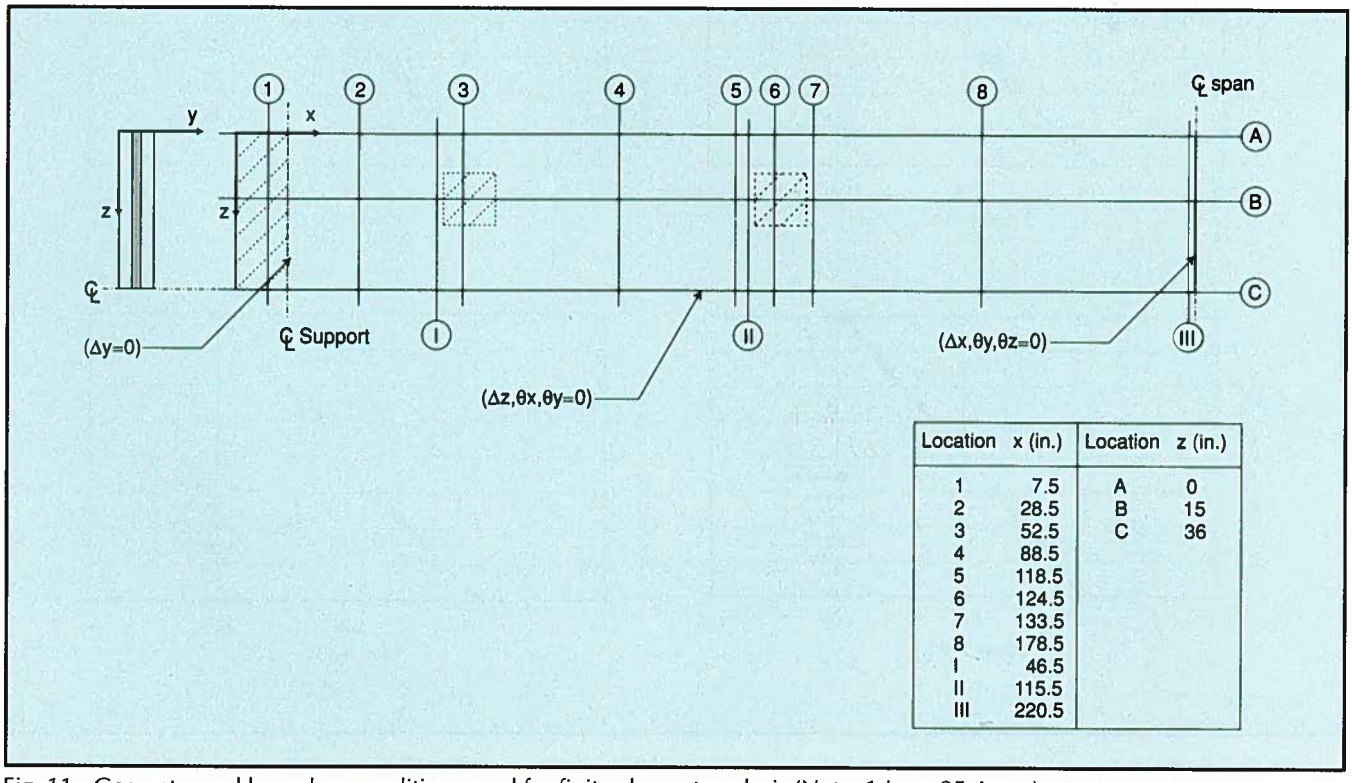

Location	x (in.)	Location	z (in.)
1	7.5	A	0
2	28.5	B	15
3	52.5	C	36
4	88.5		
5	118.5		
6	124.5		
7	133.5		
8	178.5		
I	46.5		
II	115.5		
III	220.5		

Fig. 11. Geometry and boundary conditions used for finite element analysis (Note: 1 in. = 25.4 mm).

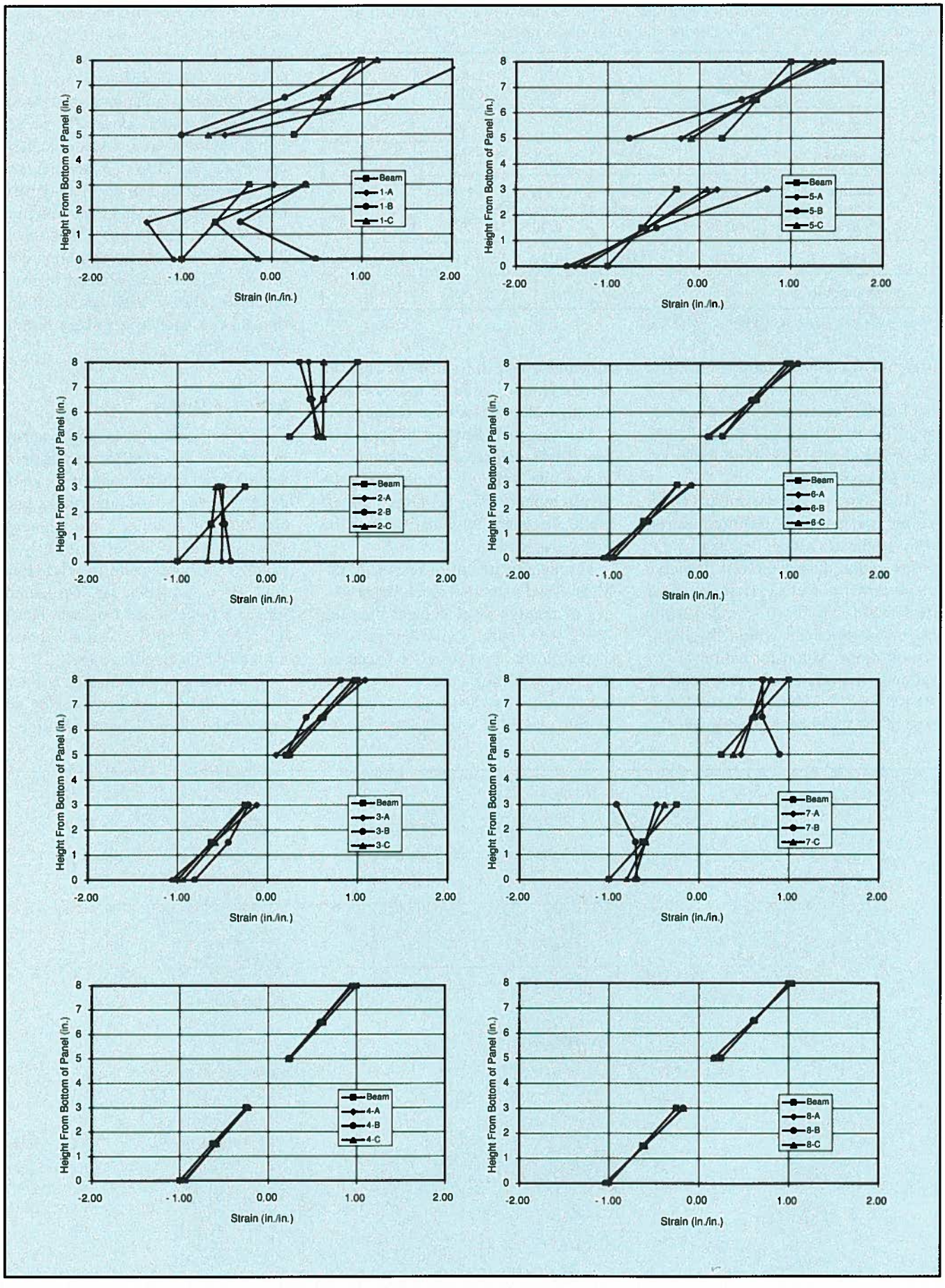

Fig. 12. Normalized strain distributions from finite element analysis of Prototype Panel at Locations 1 through 8 (Note: 1 in. = 25.4 mm).

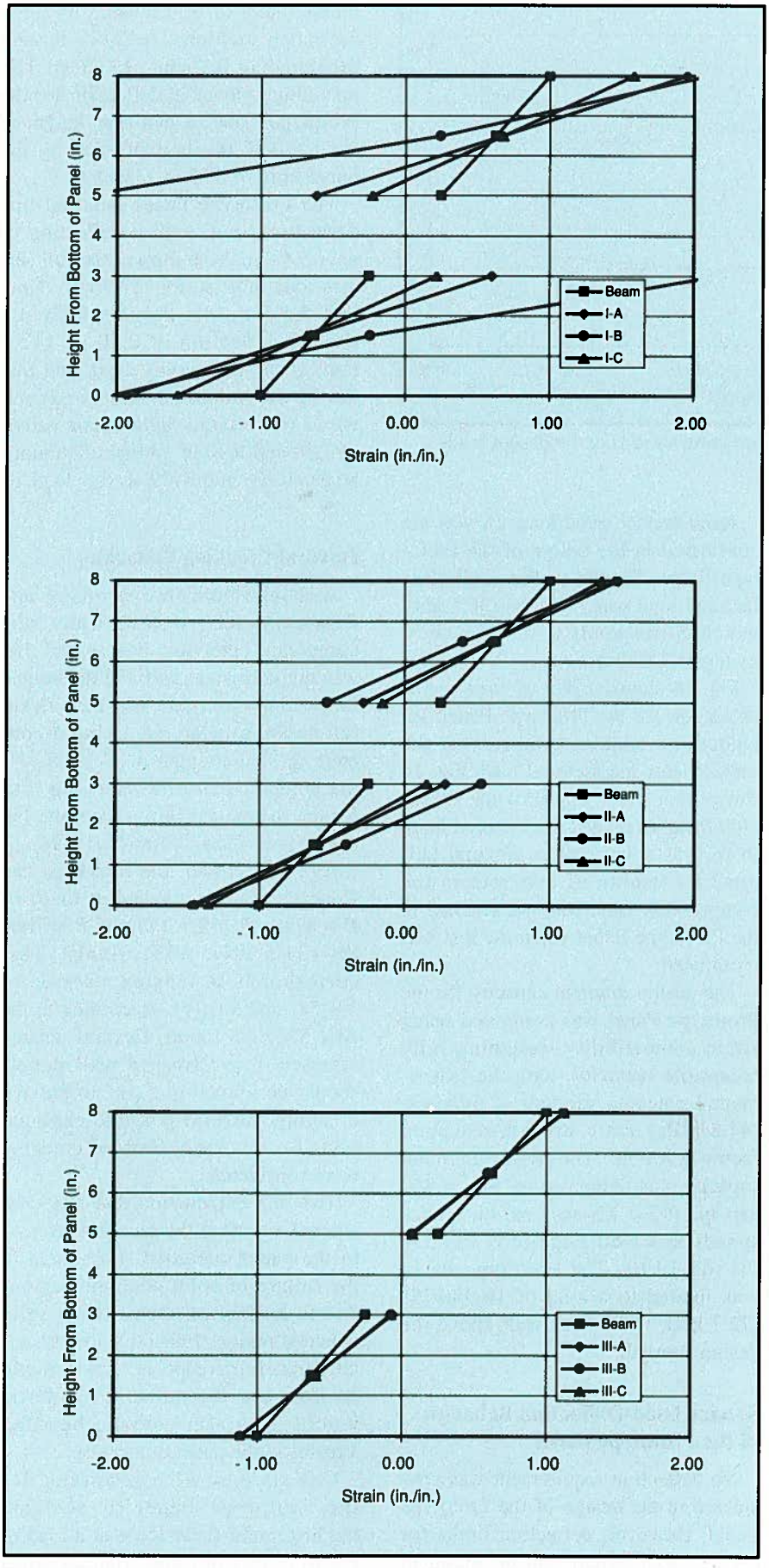

Fig. 13. Normalized strain distributions from finite element analysis of Prototype Panel at Locations I through III, the actual strain gauge locations (Note: 1 in. = 25.4 mm).

strains in the Prototype Panel under the action of lateral pressure. Fig. 11 shows the quarter symmetry model that was used in the analysis. The coordinate axes for the model are also shown in the figure.

Finite elements representing the concrete and the insulation were included in the model, with the insulation perfectly bonded to the concrete. The model comprised 5328 eight-node solid elements, with 74 elements along the x-axis, six elements along the y-axis, and 12 elements along the z-axis. All concrete elements measured $x = 3$ in. (76 mm), $y = 1.5$ in. (38 mm), $z = 3$ in. (76 mm) and all insulation elements measured $x = 3$ in. (76 mm), $y = 1$ in. (25 mm), $z = 3$ in. (76 mm). The modulus of elasticity of the concrete and insulation were 4750 and 1.35 ksi (32.8 GPa and 9.3 MPa), respectively.

Restraint conditions along the two lines of symmetry and at the support are shown in Fig. 11. Since only a linear elastic analysis was performed, the model was subjected to an arbitrary 1 psi (6.9 kPa) load, which was applied across the full width and over the entire length between the support and the midspan line of symmetry.

Fig. 12 shows the strain distributions from the finite element analysis at eight locations along the length of the panel. At each location along the length, strain distributions are plotted at three different locations across the width of the panel. These strain distributions are normalized with respect to the theoretical strain distributions, which were calculated at each location along the length, assuming a fully composite section and the same arbitrary 1 psi (6.9 kPa) load.

Consistent with beam theory, the theoretical strain distributions were assumed to be uniform across the width of the model. Each graph in Fig. 12 shows a normalized theoretical strain distribution for that location along the span, as well as the strain distributions from the finite element analysis. Each strain distribution is identified by a letter and a number, which corresponds to a location specified by the markers on Fig. 11.

Fig. 12 shows that plane sections do not exist through the entire depth of the panel at all locations along the

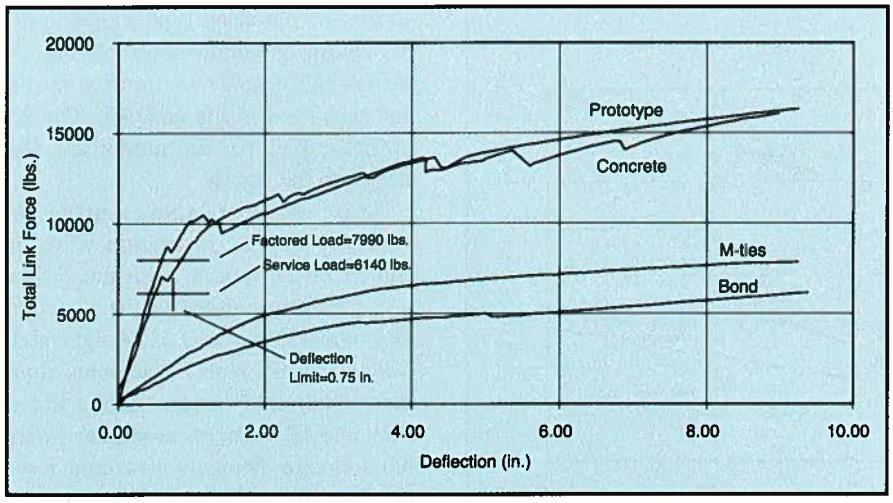

Fig. 14. Plot of load versus deflection for all test panels showing the design loads (Note: 1 in. = 25.4 mm; 1 lb = 4.448 N).

model. The figure also shows that at some locations, the strain distributions were not uniform across the width of the panel.

Fig. 13 shows the strain distributions at three locations (Locations I through III) where the strain gauges were placed on the Prototype Panel. These strain distributions also show that plane section behavior does not exist in the panel at all of the strain gauge locations, and again that the strain distributions were not uniform across the width of the panel.

Based on the results presented above, it is concluded that the strain values measured in the experiments were dependent upon the placement of the strain gauges. Therefore, the strain data obtained from the test panels appear to provide little information about the degree of composite action. However, this information may be useful in understanding the early flexural cracking that occurs in these panels. This is discussed later in the paper.

Flexural Strength of the Prototype Panel

The Prototype Panel was designed for a service pressure of W = 32 psf (1.53 kPa). For the given panel area, this corresponds to a total force P = 6140 lbs (27.3 kN). All factored load combinations were checked as required by ACI 318-99. The controlling load combination for the factored load, U, was computed as:

$$U = 0.9D + 1.3W \quad (4)$$

Axial service dead load, D, was not considered in the design of the Prototype Panel. Therefore, the controlling factored load was 7990 lbs (35.5 kN), which corresponds to a pressure of 41.6 psf (2.0 kPa).

Fig. 14 shows a plot of load versus deflection for the Prototype Panel. Included are markers representing the service load and factored load. Fig. 14 shows that the strength of the Prototype Panel exceeded the factored load. In fact, as noted earlier, flexural failure by crushing of concrete in the compression zone was not reached in the Prototype Panel when the test was terminated.

The design moment capacity for the Prototype Panel was computed using strain compatibility, assuming fully composite behavior, with the experimental concrete strength of 6930 psi (47.8 MPa) and a strength reduction factor ϕ = 0.90. The design moment capacity was computed as ϕM_n = 820 kip-in. (92.7 kN-m), which corresponds to a total force of P =14,230 lbs (63.3 kN). The Prototype Panel was loaded to a load of 16,340 lbs (72.7 kN), which was well above the design strength.

Service Load-Deflection Behavior of the Prototype Panel

No deflection requirement was considered in the design of the Prototype Panel. However, deflection limits for precast wall panels can be found in ACI 533R-93. Deflections for nonloadbearing precast wall panel elements likely to be damaged by large deflection are limited to $L/480$, but not greater than 0.75 in. (19 mm). The maximum allowable deflection for the Prototype Panel, with a span length of 35 ft (10.67 m), is controlled by the upper limit of 0.75 in. (19 mm).

The Prototype Panel satisfied this deflection limit, with a deflection of only 0.43 in. (10.9 mm) at the full service load of 6140 lbs (27.3 kN). Note that the Concrete Panel exhibited a similar deflection of 0.50 in. (12.7 mm) at the full service load, and that the M-tie and Bond Panels experienced much larger deflections values of 3.30 and 9.30 in. (84 and 236 mm), respectively, at the full service load.

Flexural Cracking Behavior

Although both the Prototype and Concrete Panels exhibited nearly fully composite behavior, one aspect that was not consistent with the theoretical fully composite panel was their flexural cracking behavior. Using a concrete tension strength of $f_r' = 7.5\sqrt{f_c'}$, the computed flexural cracking load for the theoretical fully composite behavior is P = 12,670 lbs (56.4 kN).

As noted earlier, the Prototype and Concrete Panels cracked at loads of P = 8710 lbs (38.7 kN) and P = 7080 lbs (31.5 kN), respectively. This corresponds to tension stresses of $3.8\sqrt{f_c'}$ and $3.6\sqrt{f_c'}$. According to the ACI 533R-93 report, flexural tension stresses in prestressed wall panels should be limited to $5\sqrt{f_c'}$ to prevent cracking. Several possible explanations for this early flexural cracking were considered.

The first explanation that was considered was that the bending stresses in the panel increased subsequent to the failure of solid concrete regions due to horizontal shear. If the solid concrete regions failed due to horizontal shear, full composite action would be lost, and the moment of inertia would decrease, causing bending stresses in the panel to increase.

Calculations were performed for the Prototype Panel to evaluate the horizontal shear force at a load of P = 8710 lbs (38.7 kN). The calculated horizontal shear force was then compared with the predicted horizontal

shear capacity. The horizontal shear force, H, is computed as:

$$H = \frac{\Delta M(Q)}{I_c} \quad (5)$$

where

ΔM = change in moment across the shear span
Q = first moment of inertia of the composite section
I_c = fully composite moment of inertia of the panel

The shear span is taken as one-half of the clear span of the panel. This calculation indicates that at P = 8710 lbs (38.7 kN), the horizontal shear force H = 90 kips (400 kN) in the Prototype Panel.

The horizontal shear capacity, V_{nh}, was computed according to the PCI Design Handbook as:

$$V_{nh} = 80A_{cs} \text{ (in psi)} \quad (6)$$

where A_{cs} is the total area of concrete resisting horizontal shear, sq in.

Eq. (6) assumes that the strength of unreinforced concrete due to horizontal shear is 80 psi (552 kPa). The Prototype Panel had a total area of concrete, A_{cs}, equal to 1440 sq in. (929 x 10^3 mm^2). Therefore, the Prototype Panel had a predicted horizontal shear capacity of 115 kips (512 kN).

From the calculations presented above, at first flexural cracking in the Prototype Panel, the computed horizontal shear force, H, was only 78 percent of the horizontal shear capacity. Also, it is likely that the shear strength of unreinforced concrete is actually much greater than the value of 80 psi (552 kPa). Tests performed by Hofbeck et al.[13] indicated that the shear strength of initially uncracked unreinforced concrete is approximately 500 psi (3.45 MPa). This value is much higher than 80 psi (552 kPa), and thus the actual horizontal shear capacity of the Prototype Panel is likely much higher than 115 kips (512 kN). Therefore, it is not likely that the solid regions failed, leading to a loss of horizontal shear transfer and early flexural cracking.

A second possible explanation for the early flexural cracking was that the actual stress distributions differed greatly from the distributions predicted from beam theory. Consider first the sections near the edges of the solid regions. As shown in Fig. 12, the finite element analysis results indicate that strains are especially high at Locations 5 and 7. These higher strain values indicate that stress concentrations exist at the solid concrete regions.

This can also be seen in Fig. 13 at Locations I and II. However, although several cracks did form immediately adjacent to the solid regions, these were not the first flexural cracks to form during the tests. Therefore, the early flexural cracking of the Prototype and Concrete Panels is not attributed to stress concentrations near the solid regions.

The finite element analysis results do show that the concrete stresses at midpsan, away from the solid concrete regions, are somewhat higher than those predicted by beam theory (Location III in Fig. 13). The stresses computed from finite element analysis are approximately 13 percent higher than the stresses computed using beam theory for a theoretical fully composite panel. However, the Prototype Panel cracked at a load approximately 31 percent lower than the predicted flexural cracking load. Therefore, the differences between the finite element results and beam theory do not fully explain the low cracking load behavior of the Prototype and Concrete Panels.

CONCLUSIONS

Based on the results of this study, the following conclusions are made:

1. For the panel geometries and materials treated in this study, the solid concrete regions provided most of the composite action achieved in the panels. Steel M-tie connectors and bond between the insulation and concrete contribute relatively little to composite behavior, and they should not be considered to provide composite behavior in design.

2. A precast concrete sandwich wall panel constructed similarly to the Prototype Panel treated in this study will behave as a fully composite panel in terms of service load-deflection behavior and flexural strength.

3. Panels with solid concrete regions placed intermittently along the span develop stress concentrations at the solid regions, do not exhibit plane section behavior through the depth of the panels, and develop strains that are not uniform across the width of the panels. These effects may contribute to early flexural cracking.

RECOMMENDATIONS

Based on the results of this study, the following design recommendations are made:

1. Solid concrete regions should be proportioned to provide all of the required composite action in a precast concrete sandwich wall panel. If full composite action is required at service loads, the amount and arrangement of solid concrete regions similar to the amount provided in the Prototype Panel will largely achieve this requirement. If flexural cracking at service load is a concern, allowance should be made for the expected reduced cracking stress that occurs in panels with intermittent placement of solid concrete regions along the span.

2. Alternatively, the effects of intermittent placement of the solid concrete regions may be reduced by designing a panel with a prismatic section (e.g., solid concrete ribs that run the entire span length of a panel). However, further research is needed to demonstrate that this is the case.

3. If full composite behavior is required at overload, the solid regions should be designed to provide adequate strength to resist the horizontal forces that develop at this overload, and the solid concrete regions should be arranged to minimize shear lag to ensure that the entire panel width is effective in compression. Current code approaches such as shear friction may be used to proportion the solid regions in this case.

4. One disadvantage of relying on solid concrete regions to provide composite action is that the thermal performance of the panel is adversely affected by the thermal bridges created by the solid concrete regions. In such instances, it may be required to eliminate the solid concrete regions and

provide composite action through wythe connectors and insulation. If this is the case, then the connectors and insulation should be designed specifically for that purpose.

To illustrate the above point, alternative configurations of wythe connectors, such as truss connectors, may be designed and evaluated as a means for providing composite action. Insulation materials with variable thickness (for example, stepped or corrugated profiles) that provide mechanical interlock with the concrete may be designed and evaluated as a means for providing composite action. In either case, the performance of the connector system should be verified by full-scale testing.

ACKNOWLEDGMENTS

This research was funded by the Pennsylvania Infrastructure Technology Alliance and by Lehigh University. Additional financial and technical support was provided by Composite Technologies Corporation, Dayton Superior Corporation, H. Wilden and Associates, High Concrete Structures Inc., Metromont Prestress Company, Morse Bros. Inc., Nitterhouse Concrete Products, Owens Corning, the Precast/Prestressed Concrete Institute, Stresscon Corporation, and Tindall Concrete. The support from these sponsors is gratefully acknowledged.

The authors also want to express their appreciation to the PCI JOURNAL reviewers for their thoughtful and constructive comments, which have improved the paper.

The findings and conclusions presented in this report are those of the authors, and do not necessarily reflect the views of the sponsors.

REFERENCES

1. Einea, A., Salmon, D. C., Fogarasi, G. J., Culp, T. D., and Tadros, M. K., "State-of the-Art of Precast Concrete Sandwich Panels," PCI JOURNAL, V. 36, No. 6, November-December 1991, pp. 78-98.
2. PCI Committee on Precast Sandwich Wall Panels, "State-of-the-Art of Precast/Prestressed Sandwich Wall Panels," PCI JOURNAL, V. 42, No. 2, March-April 1997, pp. 92-134.
3. PCI Committee on Precast Sandwich Wall Panels, "State-of-the-Art of Precast/Prestressed Sandwich Wall Panels," PCI JOURNAL, V. 42, No. 3, May-June 1997, pp. 32-48.
4. Pfeifer, D. W., and Hanson, J. A., "Precast Concrete Wall Panels: Flexural Stiffness of Sandwich Panels," Special Publication SP-11, American Concrete Institute, Farmington Hills, MI, March 1964, pp. 67-86.
5. Bush, T. D., Jr., and Stine, G. L., "Flexural Behavior of Composite Prestressed Sandwich Panels," M.S. Thesis, Department of Civil Engineering, University of Oklahoma, Norman, OK, 1992, 133 pp.
6. Bush, T. D., Jr., and Stine, G. L., "Flexural Behavior of Composite Prestressed Sandwich Panels with Continuous Truss Connectors," PCI JOURNAL, V. 39, No. 2, March-April 1994, pp. 112-121.
7. ACI Committee 318, "Building Code Requirements for Structural Concrete (ACI 318-99) and Commentary (ACI 318R-99)," American Concrete Institute, Farmington Hills, MI, 1999.
8. *PCI Design Handbook: Precast and Prestressed Concrete*, Fifth Edition, Precast/Prestressed Concrete Institute, Chicago, IL, 1999.
9. ACI Committee 533, "Guide for Precast Concrete Wall Panels (ACI 533R-93)," American Concrete Institute, Farmington Hills, MI, 1993.
10. Mlynarczyk, A., "Experimental Evaluation of the Composite Behavior of Precast Concrete Sandwich Wall Panels," M.S. Thesis, Department of Civil and Environmental Engineering, Lehigh University, Bethlehem, PA, August 2000.
11. Mlynarczyk, A., and Pessiki, S., "Experimental Evaluation of the Composite Behavior of Precast Concrete Sandwich Wall Panels," Report No. 00-07, Center for Advanced Technology for Large Structural Systems, Lehigh University, August 2000, 129 pp.
12. Nilson, A. H., *Design of Prestressed Concrete*, Second Edition, John Wiley and Sons, Inc., New York, NY, 1987, 592 pp.
13. Hofbeck, J. A., Ibrahim, I. O., and Mattock, A. H., "Shear Transfer in Reinforced Concrete," *ACI Journal*, V. 66, No. 2, February 1969, pp.119-128.

APPENDIX A – NOTATION

A_c = total area of concrete in cross section (both wythes)
A_{cs} = total area of concrete resisting horizontal shear
A_p = area of prestressing steel
b = width of test panel
D = dead load
e_p = eccentricity of prestressing steel
E_c = modulus of elasticity of concrete
E_{ci} = modulus of elasticity of concrete at transfer of prestress
E_p = modulus of elasticity of prestressing steel
f'_c = unconfined concrete compressive strength
f'_{ci} = unconfined compressive strength of concrete at transfer of prestress
f_{pe} = effective prestress stress in prestressing steel
f_{pi} = initial prestress stress in prestressing steel
f_{pu} = tensile strength of prestressing steel
f_{py} = yield stress of prestressing steel
f'_r = modulus of rupture of concrete
H = horizontal shear force
I_c = moment of inertia of composite concrete section
I_{cr} = moment of inertia of fully cracked section transformed to concrete
I_e = effective moment of inertia
I_{exp} = experimentally determined moment of inertia
I_g = moment of inertia of gross concrete section
I_{nc} = moment of inertia of noncomposite concrete section
L = span length of test panel
L' = length of test panel
M_a = maximum moment acting in span
M_{cr} = cracking moment
M_n = nominal moment capacity
P = total load applied to panel
P_e = effective prestress force
P_i = initial prestress force
Q = first moment of inertia
R = effectiveness ratio of prestress
S_c = section modulus of composite section
S_{nc} = section modulus of noncomposite section
U = factored load
V_{nh} = horizontal shear capacity
w = uniformly distributed load per length
W = service load wind pressure
Δ = midspan lateral deflection
ΔM = change in moment across shear span
ϕ = strength reduction factor, equal to 0.9 for bending
κ = factor to describe percent composite action of panel

APPENDIX B – DESIGN CALCULATIONS FOR PROTOTYPE PANEL

Panel Design Parameters:

Wind load = 32 psf (1.53 kPa)
Panel self-weight = 75 psf (3.59 kPa)
Assume panel behaves as 70 percent composite during service.

Allowable Tension Stresses:

The allowable tension stresses for wall panels are defined in Section 2.5.3.3 of the ACI 533R-93.[9]

Stripping and handling $= 5\sqrt{f'_{ci}}$ = 0.296 ksi (2.04 MPa)

Travel $= 5\sqrt{f'_c}$ = 0.387 ksi (2.67 MPa)

Service $= 7.5\sqrt{f'_c}$ = 0.580 ksi (4.00 MPa)

Check Stripping and Handling Stresses:

Forces imposed during stripping and handling are discussed in Section 5.2 of the PCI Design Handbook.[8]

Stripping multiplier = 1.4 (controls)
Handling multiplier = 1.2
Factored panel weight = 1.4(75) = 105 psf (5.03 kPa)

Check stress due to bending about x-axis (where the x-axis is defined as the axis along the length of the panel):

$+M_x = -M_x = 0.0054wb^2L' = 0.0054(105/1000)(6)^2(37)$
= 0.76 kip-ft
= 9.1 kip-in. (1.03 kN-m)

Resisting width of panel:
$15t = 15(8) = 120$ in.
$L/4 = 37(12)/4 = 111$ in. (controls)

Effective section modulus:
$S_{eff} = 756(111/72)$
$= 1166$ in.^{3} (19.11×10^6 mm^3)

$$f_x = -f_{pe} + \frac{M_x}{S_{eff}} = -0.350 + (9.1/1166)$$
$$= -0.342 \text{ ksi} \quad (-2.36 \text{ MPa})$$

-0.342 ksi < 0.296 ksi (OK)

Check stress due to bending about y-axis (where the x-axis is defined as the axis along the width of the panel):

$+M_y = -M_y = 0.0062wbL'^2 = 0.0062(105/1000)(6)(37)^2$
= 5.17 kip-ft
= 62.1 kip-in. (7.01 kN-m)

Resisting width of panel:
$b/2 = 72/2 = 36$ in.

Effective section modulus:
$S_{eff} = 756(36/72)$
$= 378$ in.^{3} (6.19×10^6 mm^3)

$$f_y = -f_{pe} + \frac{M_y}{S_{eff}} = -0.350 + (62.1/378)$$
$$= -0.186 \text{ ksi} \quad (-1.28 \text{ MPa})$$

-0.342 ksi < 0.296 ksi (OK)

Check Travel Stresses:

Forces imposed during travel are also discussed in Section 5.2 of the PCI Design Handbook.

Stripping multiplier = 2.0 (more conservative than PCI value of 1.5)

Factored panel weight = 1.4(75) = 150 psf (7.18 kPa)

Check stress due to bending about x-axis:
$+M_x = -M_x = 0.0054wb^2L' = 0.0054(150/1000)(6)^2(37)$
= 1.08 kip-ft
= 12.9 kip-in. (1.46 kN-m)

$$f_x = -f_{pe} + \frac{M_x}{S_{eff}} = -0.350 + (12.9/1166)$$
$$= -0.339 \text{ ksi} \quad (-2.34 \text{ MPa})$$

-0.339 ksi < 0.387 ksi (OK)

Check stress due to bending about y-axis:

$+M_y = -M_y = 0.0062wbL'^2 = 0.0062(150/1000)(6)(37)^2$
= 7.63 kip-ft
= 91.7 kip-in. (10.36 kN-m)

$$f_y = -f_{pe} + \frac{M_y}{S_{eff}} = -0.350 + (62.1/378)$$
$$= -0.186 \text{ ksi} \quad (-1.28 \text{ MPa})$$

-0.186 ksi < 0.387 ksi (OK)

Nominal Moment Capacity:

The nominal moment capacity of the section is computed using the equation for f_{ps}, given in Section 18.7.2 of the ACI Building Code (ACI 318-99).

$$f_{ps} = f_{pu}\left[1 - \frac{\gamma_p}{\beta_1}\left(\rho_p \frac{f_{pu}}{f'_c}\right)\right], \quad \text{where } \gamma_p = 0.28 \text{ and } \beta_1 = 0.75$$

$f_{ps} = f_{pu}(1 - 16.8\rho_p)$

Assuming noncomposite action:

$$\rho_p = \frac{A_p}{bd_p} = \frac{0.46}{72(1.5)} = 0.00426$$

$f_{ps} = 250.7$ ksi

$$a = \frac{A_p f_{ps}}{0.85 f'_c b} = \frac{0.46(250.7)}{0.85(6)(72)} = 0.31 \text{ in.}$$

$$\phi M_n = \phi A_p f_{ps}(d_p - \frac{a}{2})$$
$$= 0.9(0.46)(250.7)(1.5 - \frac{0.31}{2})$$

$$= 140.1 \text{ kip-in.} \quad (15.83 \text{ kN-m})$$

$\phi M_n = 280$ kip-in. (31.64 kN-m) for two wythes

Assuming composite action:

$$\rho_p = \frac{A_p}{bd_p} = \frac{0.92}{72(4)} = 0.00320$$

$f_{ps} = 255.5$ ksi

$$a = \frac{A_p f_{ps}}{0.85 f'_c b} = \frac{0.92(255.5)}{0.85(6)(72)} = 0.64 \text{ in.}$$

$$\phi M_n = \phi A_p f_{ps}(d_p - \frac{a}{2})$$
$$= 0.9(0.92)(255.5)(4 - \frac{0.64}{2})$$

$$= 778 \text{ kip-in. } (87.91 \text{ kN-m})$$

Design moment capacity of 70 percent composite panel:
$\phi M_n = 0.70(778 - 280) + 280 = 629$ kip-in. (71.08 kN-m)

Cracking Moment:

As given by Section 18.8.3 of ACI 318-99, the design flexural strength must be at least 1.2 times the cracking strength.

Section properties for 70 percent composite panel:
$I_{pc} = 0.70(3024 - 324) + 324 = 2214$ in.^{4} (922×106 mm^4)
$S_{pc} = 2214/4 = 553$ in.^{3}

$$M_{cr} = (f'_r + f_{pe})S_{pc} = (0.58 + 0.35)(553)$$
$$= 514 \text{ kip-in.} \quad (58.08 \text{ kN-m})$$

Check $\phi M_n > 1.2 M_{cr}$
$\phi M_n / M_{cr} = 629/514 = 1.2$ (OK)

Ultimate Moment:

$U = 0.9D + 1.3W = 1.3(32) = 41.6$ psf (1.99 kPa)
$w = 41.6(6) = 250$ lbs/ft $= 0.021$ kip/in. (3.68 kN/m)

$$M_u = \frac{wL^2}{8} = \frac{0.021(35 \times 12)^2}{8} = 463 \text{ kip-in.} \quad (52.32 \text{ kN/m})$$

$\phi M_n > M_u$ (OK)

Check Service Stresses:

$w = 32$ psf(6 ft) $= 192$ lbs/ft $= 0.016$ kip/in. (2.80 kN/m)

$$M_s = \frac{wL^2}{8} = \frac{0.016(35 \times 12)^2}{8} = 353 \text{ kip-in.} \quad (39.89 \text{ kN-m})$$

$$f_s = -f_{pe} + \frac{M_s}{S_{pc}} = -0.350 + (353/553)$$
$$= 0.288 \text{ ksi} \quad (1.99 \text{ MPa})$$

0.288 ksi < 0.580 ksi (OK)

Check Capacity of Solid End Regions Using Shear Friction:

The horizontal shear strength of the solid end regions of the panel is computed using the equation for V_n, given in Section 11.7 of ACI 318-99.

$$\phi V_n = A_{vf} f_y \mu = 0.85(0.78)(60)(1.4 \times 1.0)$$
$$= 55.7 \text{ kips} \quad (247.8 \text{ kN})$$

$\mu = 1.4\lambda$ for concrete placed monolithically

$\lambda =$ for normal weight concrete

$$\phi V_n < \phi 0.2 f'_c A_c = 0.85(0.2)(6000)(72 \times 12)$$
$$= 881{,}280 \text{ lbs} = 881 \text{ kips} \quad (3918 \text{ kN}) \quad \text{(OK)}$$

$$\phi V_n < \phi 800 A_c = 0.85(800)(72 \times 12)$$
$$= 587{,}520 \text{ lbs} = 588 \text{ kips} \quad (2615 \text{ kN}) \quad \text{(OK)}$$

$$V_u = \frac{wL}{2} = \frac{0.021(35 \times 12)}{2} = 4.41 \text{ kips} \quad (19.6 \text{ kN})$$

$\phi V_n > V_u$ (OK)